J. Cosmet. Sci., 66, 95–111 (March/April 2015)

Optimal aluminum/zirconium: Protein interactions for predicting antiperspirant efficacy using zeta potential measurements

SHAOTANG YUAN, JOHN VAUGHN, IRAKLIS PAPPAS, MICHAEL FITZGERALD, JAMES G. MASTERS, and LONG PAN, *Colgate-Palmolive Company Piscataway, NJ 08854*

Accepted for publication February 11, 2015

Synopsis

The interactions between commercial antiperspirant (AP) salts [aluminum chlorohydrate (ACH), activated ACH, aluminum sesquichlorohydrate (ASCH), zirconium aluminum glycine (ZAG), activated ZAG], pure aluminum polyoxocations (Al_{13}-mer, Al_{30}-mer), and the zirconium(IV)–glycine complex $\left[Zr_6(O)_4(OH)_4(H_2O)_8(Gly)_8\right]^{12+}$ (CP-2 or ZG) with Bovine serum albumin (BSA) were studied using zeta potential and turbidity measurements. The maximal turbidity, which revealed the optimal interactions between protein and metal salts, for all protein–metal salt samples was observed at the isoelectric point (IEP), where the zeta potential of the solution was zero. Efficacy of AP salts was determined via three parameters: the amount of salt required to flocculate BSA to reach IEP, the turbidity of solution at the IEP, and the pH range over which the turbidity of the solution remains sufficiently high. By comparing active salt performance from this work to traditional prescreening methods, this methodology was able to provide a consistent efficacy assessment for metal actives in APs or in water treatment.

INTRODUCTION

Charge neutralization (coagulation) and sweep flocculation are well-known mechanisms of action between cationic coagulants and organic matter in the treatment of waste water (1,2). Salts of aluminum such as aluminum polyoxocations, aluminum chlorohydrate (ACH), or aluminum chloride ($AlCl_3$) are often selected to treat waste water because they exhibit strong coagulation and flocculation behavior (3–6). Besides water treatment and many other applications, these salts are the predominant active ingredients employed in antiperspirant (AP) formulations, which reduce more than 20% perspiration and show considerable odor inhibition in the underarm area (7,8). "Plug Theory," a well-known theory of sweat reduction proposed by Reller and Luedders (9), postulates that dissolved AP salts diffuse into the sweat duct and are hydrolyzed upon contacting with sweat to form an amorphous metal hydroxide plug that physically blocks the escape of sweat from

Address all correspondence to Long Pan at long_pan@colpal.com.

the duct. On the basis of the plug model, it is clear that the efficacy of AP salts critically dependents on the speed and depth with which the salt penetrates into the sweat glands to form a strong plug—deeper and less superficial plugs will be more substantive (10–14). Bearing this in mind, actives of a smaller particle size should show better efficacy. Consequently, the assessment of AP efficacy lies mostly in particle size analysis, i.e., size-exclusion chromatography and light scattering.

In addition to Plug Theory, other interpretations of this process are also plausible. For instance, previous research has investigated the interaction and formation of floc between metal cations or complexes and biomolecules (15–21). Since biomolecules (e.g., proteins) are important components of sweat (22), it is also conceivable that metal ions of AP salts react with the biomolecules in sweat to form water-insoluble complexes, which in turn triggers plug formation in the sweat gland. This mechanism would be similar to the mechanism of coagulation and flocculation in water treatment. These interactions between metal cationic species and biomolecules can be analyzed by zeta potential (ζ-potential) characterization, which is a powerful technique in the evaluation of coagulant agents in water treatment (13,23–26).

ζ-Potential is the surface charge of a particle in a colloid system, and is a strong indicator for floc formation (23–28). Isoelectric point (IEP) or point of zero charge is the pH at which the solution has a zero ζ-potential. At this point, the lack of repulsive forces between dissolved substances and suspended colloids induces coagulation and precipitation (24). Gauckler and coworkers (27) proposed a two-step adsorption of bovine serum albumin (BSA) onto Al_2O_3 particles surface by ζ-potential measurement. Another study by Perry and coworkers (16) also used ζ-potential to demonstrate the interaction of aluminum polyoxocations (Al_{13}-mer and Al_{30}-mer) with BSA or lysozyme. However, to date, the critical coagulation ratios between commercial APs and a representative protein (BSA) have not been systematically characterized by using ζ-potential measurement.

In this report, we present what's believed to be the first study of commercial AP actives and BSA by using ζ-potential and turbidity measurements with a focus on the formation of insoluble AP–BSA complexes at the pH where ζ-potential of the solution is zero, and we use the term IEP to indicate this pH of AP–BSA complex under our experiment condition. We envision a critical ratio of polycation/protein characterized by the point where the ζ-potential of the system is zero. This ratio governs the precipitation process due to the optimal interaction between protein and AP salts, and would serve as an indicator of the efficacy of the species in question. The goal of this work is to explore the possibility of using ζ-potential as a means to predict the efficacy of AP actives and other simple Al or Zr salts and to guide us to develop more efficacious AP salts. We also note that the proposed mechanism of plug formation with proteins in the sweat duct is very similar to the accepted mechanism of coagulation and flocculation in primary water treatment.

MATERIALS AND METHODS

BSA and glycine were purchased from Sigma-Aldrich (St. Louis, MO). ACH, [$Al_2(OH)_5Cl{\cdot}H_2O$, 81.6% actives, 25.2% Al] and activated ACH, [$Al_2(OH)_5Cl{\cdot}H_2O$, 82% actives, 25.4% Al]; aluminum sesquichlorohydrate (ASCH), [$Al_2(OH)_{4.8}Cl_{1.2}{\cdot}H_2O$,

82% actives, 24.3% Al]; aluminum zirconium glycine (ZAG) ($Al_{3.6}ZrCl_{3.3}(OH)_{11.5}$·Gly, 77% actives, 14.9% Al, 14.2% Zr) and activated ZAG ($Al_{3.6}ZrCl_4(OH)_{10.8}$·Gly, 74% actives, 13.9% Al, 13.3% Zr) were purchased from Summit (Huguenot, NY). Zirconium dichloride oxide, aluminum nitrate and aluminum chloride were purchased from Alfa Aesar (Ward Hills, MA). Concentrated hydrochloric acid, sodium carbonate and sodium hydroxide were purchased from J. T. Baker (Phillipsburg, NJ). The weight percentage active and metal in the AP salts were provided by the certificates of analysis from suppliers.

ZG (zirconium (IV)–glycine complex, $[Zr_6(O)_4(OH)_4(H_2O)_8(Gly)_8]$·12Cl·8$H_2O$, 88.74% actives, 29.59% Zr), was prepared according to previous procedures (29) with slight modification. Briefly, 120 mmol of zirconium dichloride oxide octahydrate ($ZrOCl_2$·8H_2O) and 177 mmol of glycine were placed in a flask with 500 ml deionized (DI) water. Concentrated HCl (4.5 ml, 33% wt) was added into this solution. The mixture was heated under reflux at 80°C under vigorously stirring for 20 h. The product was collected as an off-white powder via freeze-drying. Powder X-ray diffraction analysis was performed to confirm that the ZG powder was identical to the one reported in the literature (29).

Al_{13}-mer, $AlO_4Al_{12}(OH)_{24}(H_2O)_{12}(NO_3)_7$ (80.09% actives, 23.8% Al), was prepared following the previous literature (30) and was confirmed by both (27)Al nuclear magnetic resonance (NMR) (Al_{Td}: δ = ~63ppm) and dynamic light scattering (0.5 nm radii) (17). The Al_{13}-mer was prepared by adding 300 ml of a 0.6M Na_2CO_3 solution dropwise into 300 ml of 0.5 M $Al(NO_3)_3$·9H_2O solution at 75°C under vigorous stirring over a 3-h period. The hydrolysis ratio of $[OH^-]/[Al^{3+}]$ was 2.46. The reaction was then cooled to room temperature and allowed to sit overnight. Slight white precipitate was removed by filtration. The filtrate was freeze-dried to remove water, and a white powder was collected (30).

Al_{30}-mer, $Al_{30}O_8(OH)_{56}(H_2O)_{24}Cl_{18}$ (80.74% actives, 27.3% Al), was prepared following the previous literature (32) and was confirmed by both (27) Al NMR (Al_{Td}: δ = 70 ppm) and dynamic light scattering (1.0 nm radii) (17). The Al_{30}-mer was prepared by dropwise addition of 2 M NaOH solution into a 0.3 M $AlCl_3$ solution at 95°C under fast stirring. The hydrolysis ratio of $[OH^-]/[Al^{3+}]$ was 2.40. After the addition of NaOH, the solution was heated and stirred at 95°C for 48 h. The product was freeze-dried to remove water and a white powder was collected (31,32).

ZG, Al_{13}-mer, and Al_{30}-mer were prepared by Colgate-Palmolive (Piscataway, NJ). Weight percentage active of these three compounds were calculated based on metal, OH or O, and Cl contents.

PREPARATION OF PURE BSA, PURE AP, AND AP–BSA MIXTURE SOLUTIONS

BSA solutions of 1, 5, 10, 20, and 40 mg/ml were prepared by dissolving 100, 500, 1000, 2000, and 4000 mg solid BSA, respectively, in 100 ml of DI water. 1 mg/ml of AP solution was prepared by dissolving 100 mg of solid AP salt in 100 ml of DI water.

Different molar ratios of AP–BSA solutions were prepared by combining varying amounts of solid AP salts with 18 ml of 20 mg/ml BSA solution in vials. A white homogenous suspension was formed immediately upon certain ratio.

ZETA POTENTIAL MEASUREMENTS

All measurements of ζ-potential were conducted by using a Zetasizer Nano series from Malvern Instruments (Worcs, U.K.) equipped with an MPT-2 Autotitrator. In this instrument, ζ-potential is determined by measuring the electrophoretic mobility of particles and then calculating via the Henry Equation

$$U_E = \frac{2\varepsilon\zeta f(ka)}{3\eta}$$

where U_E is the electrophoretic mobility, ζ is the zeta potential, ε is the dielectric constant, and it is set as 78.5 by the instrument, f(ka) is Henry's function, it is set to be 1.5 automatically by Smoluchowski approximation, and η is the viscosity of the solvent (water) (33).

ζ-Potential of all solutions was measured directly after pure solutions and AP–BSA mixture solutions were prepared. Each solution (1 ml) was transferred into a cell for measurement. Universal Dip Cell (ZEN1002, Malvern Instruments) and disposable sizing cell (DTS0012, Malvern Instruments) were used for measurements of pure BSA solution, pure AP salt solutions, and AP–BSA mixture solutions without pH control. Disposable Zeta Cell (DTS1061, Malvern Instruments) was used for zeta potential measurement in pH-controlled experiments. pH of mixture solutions was adjusted via MPT-2 Autotitrator (Malvern Instruments) with 1.0 M HCl and 1.0 M NaOH solutions by Malvern Zetasizer software.

ELEMENTAL ANALYSIS

According to the molar ratio at IEP reported in this study, 18.0 ml of ACH–BSA, ZAG–BSA, Al_{13}–BSA, and ZG–BSA solutions were prepared. The mixtures were centrifuged at 5000 rpm for 15 min. The supernatant was decanted and 18.0 ml of DI water was used to wash the precipitate, followed by centrifuging at the same settings. This wash procedure was repeated three times to remove any free metal salts or BSA particles. The white AP–BSA product was freeze-dried to remove all water. C, H, and N were analyzed via Perkin-Elmer 2400 Elemental Analyzer (Waltham, MA). Metal components were analyzed by using Perkin-Elmer ICP-OES (inductively coupled plasma optical emission spectrometry) Optima 4300 DV.

TURBIDITY MEASUREMENTS

The turbidity of every mixture solutions as measured right after they were prepared by using 2100P Tubidimeter from HACH (Loveland, CO). Turbidity of AP–BSA mixture solutions was outside the range of the instrument and were thus measured by diluting 1 ml of these mixture solutions into 15 ml DI water. Turbidity of pure BSA and individual AP solutions used in the first section of experiment (zeta potential properties of individual BSA and AP solutions with pH control) were measured without dilution.

RESULT AND DISCUSSIONS

ZETA POTENTIAL AND TURBIDITY PROPERTIES OF INDIVIDUAL BSA AND AP SOLUTIONS WITH PH CONTROL

The ζ-potential and turbidity properties of pure BSA and AP solutions were studied in a pH range of 3 to 12, and the results are shown in Figure 1. Table I summarizes the important parameters found in this study. The original pH of BSA, activated ACH, ZAG, Al_{13}, and ZG were 7.04, 4.73, 4.14, 4.62, and 2.99, respectively. All solutions appeared transparent at their original pH due to the strong repulsion force between the highly charged particles.

The IEP of BSA was measured to be 4.7, which is in agreement with the value previously reported (34). The onset of precipitation is taken as the point where the turbidity is 50 NTU. The formation of visual precipitate was observed at the IEPs for all samples with the exception of BSA. However, a relatively maximum turbidity was measured for BSA at its IEP compared with other pH. For AP solutions, all IEPs fell at more basic pH.

At low pH, polycations are the main species in AP solutions (35–39), which leads to a positive ζ-potential and low turbidity. The turbidity of AP solutions increases as the pH is raised. The formation of precipitate is most likely due to the formation of aluminum hydroxide or zirconium hydroxide when pH is raised to 5 or above (35,36):

$$Al^{3+} + 3OH^- \rightarrow Al(OH)_3,$$

$$Zr^{4+} + 4OH^- \rightarrow Zr(OH)_4,$$

As the pH continues to increase, ACH and Al_{13} solutions once again become clear due to the formation of the water soluble $Al(OH)_4^-$ species (35). This transition is not observed in Zr-containing AP solutions (ZAG and ZG) because the insoluble $Zr(OH)_4$ species is predominant.

EFFECT OF AP ADDED ON ZETA POTENTIAL AND TURBIDITY OF SOLUTIONS

AP polycations are adsorbed onto the surface of BSA via electrostatic interaction with the negatively charged asparagine and glutamine side chains of BSA (34). The adsorption of AP polycations onto the BSA surface changes the ζ-potential of the AP–BSA mixture solution from negative to positive with increasing AP dosage (16).

To ascertain the amount of AP needed to make AP–BSA solutions possess a zero ζ-potential value, the ζ-potential was monitored while BSA solution was titrated with solid AP salts. Figure 2 shows turbidity as a function of ζ-potential and ACH concentration in ACH–BSA mixture. All AP salts show similar behavior (see Figure 3 for details). ζ-Potential increases with increasing AP concentration in solution. As the amount of AP solution increases, the mixture becomes cloudy due to the formation of charge-neutral AP–BSA complexes. As expected, the maximum turbidity is achieved at the pH where ζ-potential was zero (IEP), which indicates the optimal interaction between BSA and AP actives. At high levels of AP, the turbidity dissipates possibly resulting from charge reversal of the AP–BSA complex.

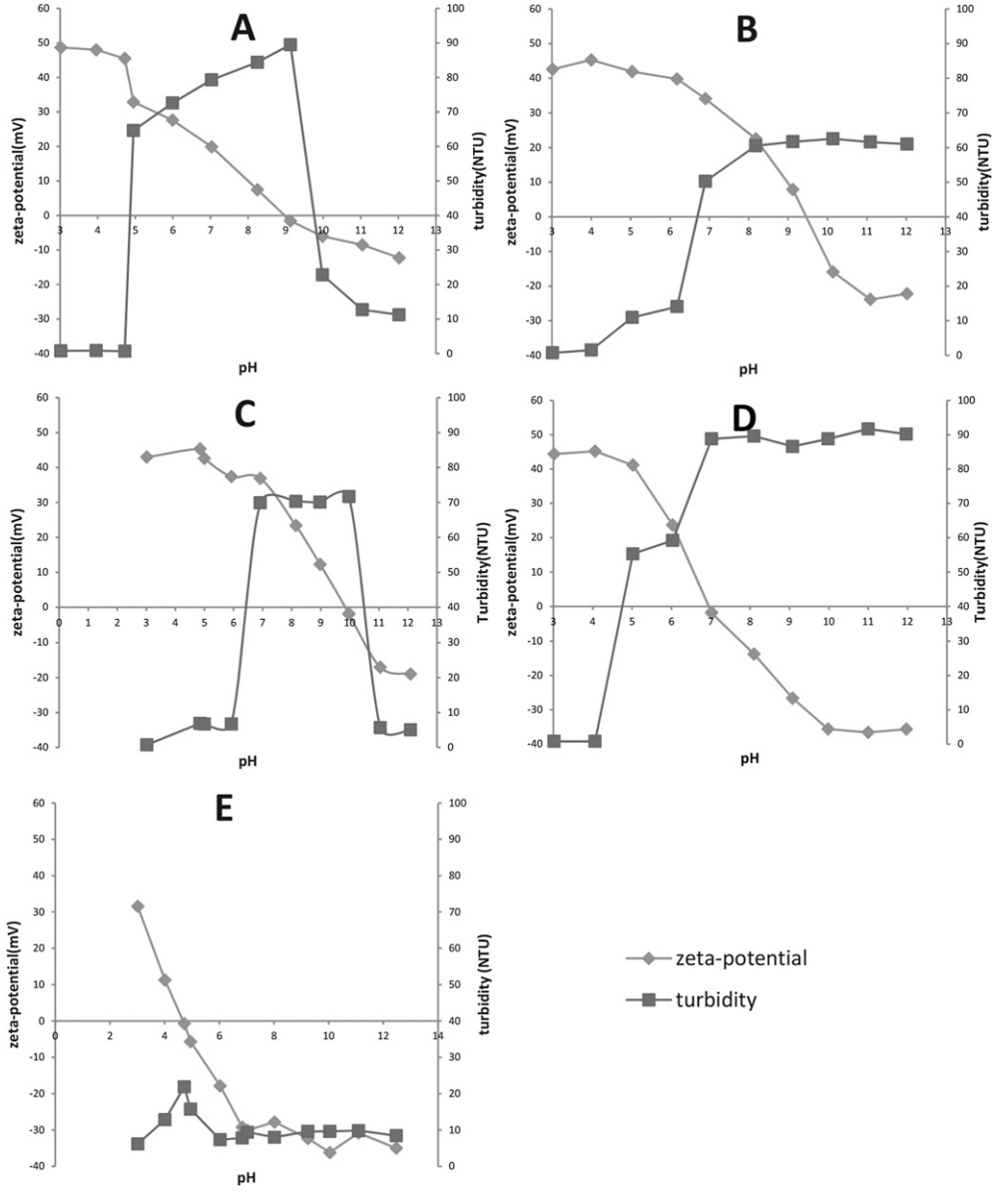

Figure 1. Zeta potential and turbidity trend of selected AP solutions and BSA solution in pH range from 3 to 12, (A) activated ACH: precipitate formed when pH>5; IEP was around 9, where turbidity of solution reached its maximum; precipitate disappeared when pH>9. (B) ZAG: precipitate formed when pH>5; IEP was around 9.5, where turbidity of solution reached its maximum; precipitate did not dissolve with further addition of base. (C) Al_{13}-mer: precipitate formed when pH>6; IEP was around 10, where turbidity of solution reached its maximum; precipitate disappeared when pH>10. (D) ZG; precipitate formed when pH>4; IEP was around 7, where turbidity of solution reached its maximum; precipitate did not dissolve with further addition of base. (E) BSA: IEP was around 4.7, where turbidity of solution reached its maximum; no precipitate was observed during titration process.

Table II summarizes the IEP values, molar ratios at IEP, maximum turbidity at IEP, as well as the dosage ranges for precipitation of four AP–BSA mixture solutions. The onset of precipitation is taken as the point where the turbidity is 50 NTU. Elemental analysis (EA) was

Table I
Concentration, Isoelectric Points, Highest Turbidity and Precipitate pH Range of Individual BSA and AP Solutions

Samples	Metal concentration (M)	IEP	Optimum turbidity* (NTU)	Precipitation pH range
activated ACH	0.0094	9.21	89.5	$5 \leq pH \leq 9$
ZAG	0.0071**	9.48	62.5	$pH \geq 7$
Al_{13}	0.0090	10.02	71.7	$7 \leq pH \leq 10$
ZG	0.0032	7.01	89.6	$pH \geq 6$
BSA	-	4.72	21.9	-

*The highest turbidity was found at IEP.
**Metal concentration of ZAG was the sum of Al and Zr.

performed on all precipitates formed at the IEP. Table III summarizes the analyzed results of percentage of C, H, N, and metal in the complexes. The calculated percentage of metal(s) in the precipitate based on the reported molar ratios is compared with the percentage of metal(s) from EA results. The decrease of C, H, and N ratios compared with pure BSA and the high correlation between calculated and obtained percentage of metal(s) in complexes confirm the formation of a substantive insoluble complex containing both BSA and AP. In addition, the correlation indicates that all added AP is bound to BSA.

Looking carefully at Tables II and III, it is apparent that the amount of ZAG needed to reach the IEP is less than half that of activated ACH. A similar trend is observed in a comparison of the single species polycations, ZG and Al_{13}-mer. The variation in AP–BSA molar ratio at the IEP is a direct indicator of the charge-neutralization capability of the AP active. Actives with a low size/charge ratio, such as ZG, precipitate BSA more readily and at a lower concentration.

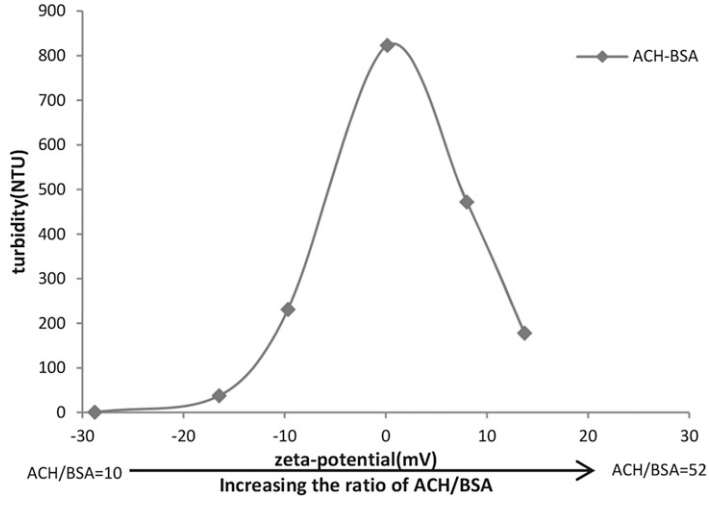

Figure 2. Turbidity of activated ACH–BSA changes as a function of zeta potential change with the increasing of activated ACH/BSA ratio. Zeta potential of solutions increased as more activated ACH was added; turbidity was firstly increased, and then decreased with the addition of activated ACH into BSA. Highest turbidity of mixture solutions were found at IEPs. ZAG, Al_{13}, and ZG all behaved the same as activated ACH.

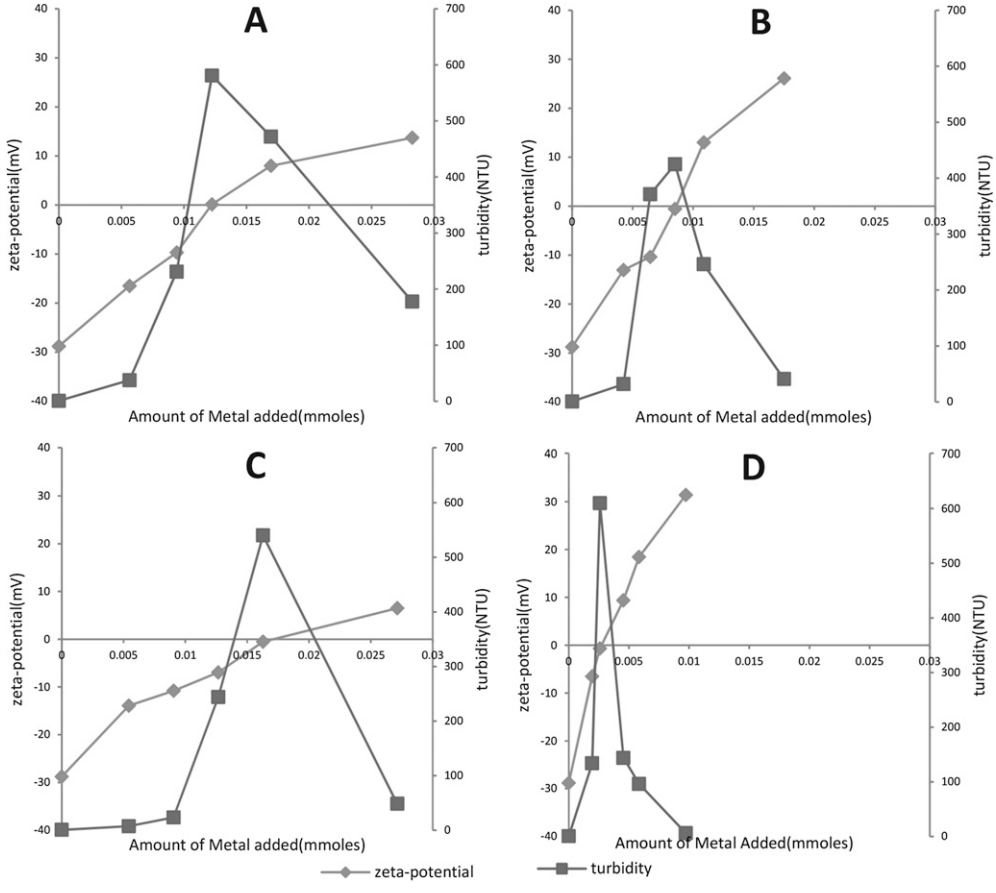

Figure 3. Zeta potential and turbidity trend of four AP-BSA mixture solutions. Zeta potential increased due to the positively charged AP particles adsorbed onto BSA particle surface. Mixture solutions changed from transparent to cloudy then transparent with increasing amount of AP added into BSA. (A) Activated ACH-BSA: when 122.4×10^{-4} mmole metal was used, IEP was found at 5.65, where turbidity reached maximum. (B) ZAG-BSA: when 85×10^{-4} mmole metal was used, IEP was found at 5.60, where turbidity reached maximum. (C) Al_{13}-BSA: when 162.79×10^{-4} mmole metal was used, IEP was found at 5.62, where turbidity reached maximum. (D) ZG–BSA: when 25.95×10^{-4} mmol metal was used, IEP was found at 5.15, where turbidity reached maximum.

Figure 4 shows a comparison of turbidity at the IEPs of pure AP solutions versus AP–BSA mixtures. Compared with the AP solutions alone, the turbidity of AP–BSA mixtures are significantly higher. There is a clear difference in the volume of precipitate when an AP is combined with BSA compared with an AP alone. This dramatic difference implicates the AP/protein floc to enhance plug forming during AP action.

MECHANISTIC STUDY

ζ-Potential experiments from the previous sections showed substantive evidence for charge neutralization in the AP–BSA interaction leading to precipitation. To understand whether sweep flocculation is also involved, a mechanistic study was designed: BSA

Table II
Isoelectronic Point, Molar Ratio of AP/BSA at IEP, Maximum Turbidity of AP–BSA Mixtures, and Precipitation Dosage Range for Four AP–BSA Samples

Samples	IEP*	Molar ratio at IEP (AP–BSA)	Turbidity at IEP (NTU)	Dosage range for precipitation* (AP–BSA molar ratio)
Activated ACH	5.60	24:1	549	$14 \leq AP/BSA \leq 62$
ZAG	5.65	8:1	392	$5 \leq AP/BSA \leq 17$
Al_{13}	5.6	4:1	525	$3 \leq AP/BSA \leq 7$
ZG	5.10	1.5:1	390	$0.5 \leq AP/BSA \leq 3$

*The dosage range is determined at the molar ratio where turbidity is greater than 50NTU.

solutions with varying concentrations were titrated by the addition of solid AP salts. The molar ratio of AP–BSA at the point of maximum turbidity was measured for each BSA concentration.

Figure 5 demonstrates the relationship between the amount of AP actives added and BSA solution in different concentrations. The linearity indicates that precipitation is governed solely by a constant AP/BSA molar ratio. Since sweep flocculation would entail the entrapment of multiple BSA molecules in a single metal hydroxide floc, this clean linear relationship argues strongly against the dominance of such a mechanism. As activated ACH, ZAG, Al_{13}, and ZG all have same performance in this study; we surmise that charge neutralization is the dominant mechanism regulating the AP–BSA interaction and plug formation.

EFFECT OF PH ON ZETA POTENTIAL AND TURBIDITY OF AP–BSA COMPLEX

We have demonstrated that ζ-potential measurements can be used to evaluate the formation of precipitate between various AP salt solutions and BSA. pH is another significant factor (39) that has effect on these systems, undoubtedly. The following studies were designed to provide insight into how the formation of precipitate was affected by varying

Table III
Comparison of Calculated Metal Percentage (w/w) in AP–BSA Complexes to the Metal Percentage Obtained from Elemental Analysis

Samples	Molar ratio at IEP (AP/BSA)	%C Obtained (w/w)	%H Obtained (w/w)	%N Obtained (w/w)	%Metal(s)	
					Calculated (w/w)	Obtained (w/w)
BSA	-	50.75	7.28	15.28	-	-
Activated ACH	24:1	49.20	7.09	14.42	1.65, Al	1.62, Al
ZAG	8:1	49.15	7.08	14.23	0.97, Al; 0.92, Zr	0.92, Al; 0.88, Zr
Al_{13}	4:1	49.08	7.12	14.43	1.79, Al	1.57, Al
ZG	1.5:1	49.86	7.13	14.67	1.27, Zr	1.70, Zr

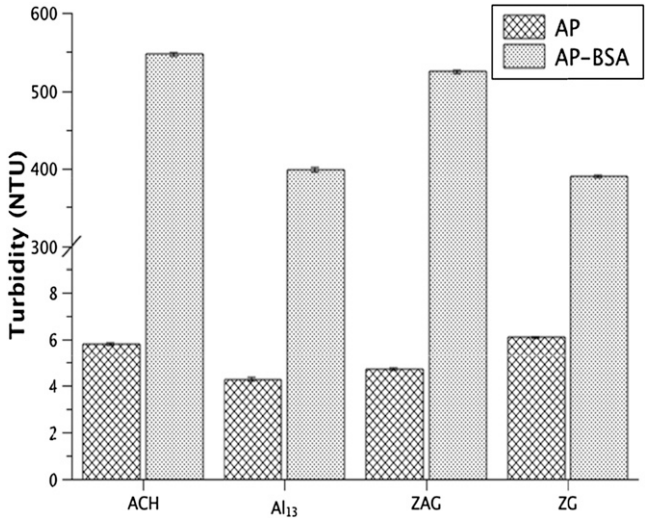

Figure 4. Comparison of maximum turbidity at IEP of pure AP solutions with AP–BSA mixture solutions. The turbidity of all solutions was measured after the dilution of 15 times.

pH. The starting mixtures were prepared according to the molar ratios at the IEP of each AP–BSA solution as demonstrated previously. ζ-Potential and turbidity measurements were performed as the pH is adjusted to the range of 3 to 11. The ζ-Potential and turbidity of all solutions varied as pH changed. Figure 6 represents the turbidity of ACH–BSA

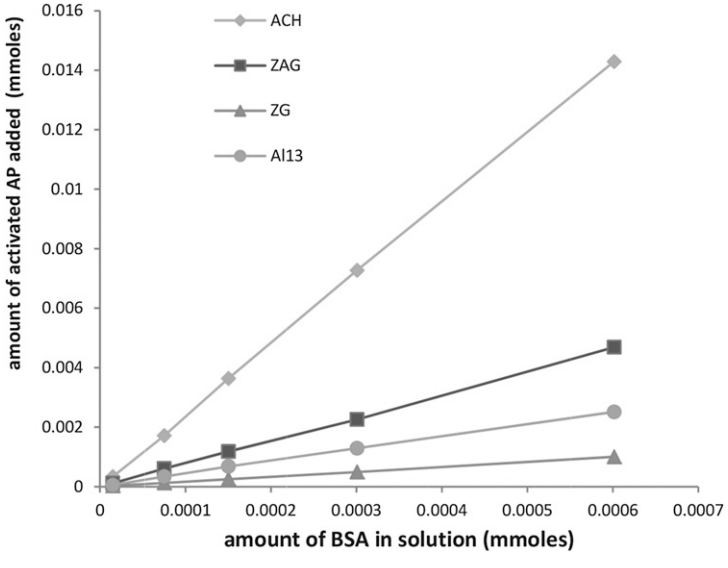

Figure 5. Amount of AP actives added as a function of BSA concentration. BSA solutions with five different concentrations (1, 5, 10, 20, and 40 mg/ml) were used. The amount of AP actives required to neutralize BSA increased the same as the ratio increases in the concentration of BSA solutions resulting in a constant value of AP/BSA ratio. Activated ACH, ZAG, Al_{13}, and ZG had same behavior under this study.

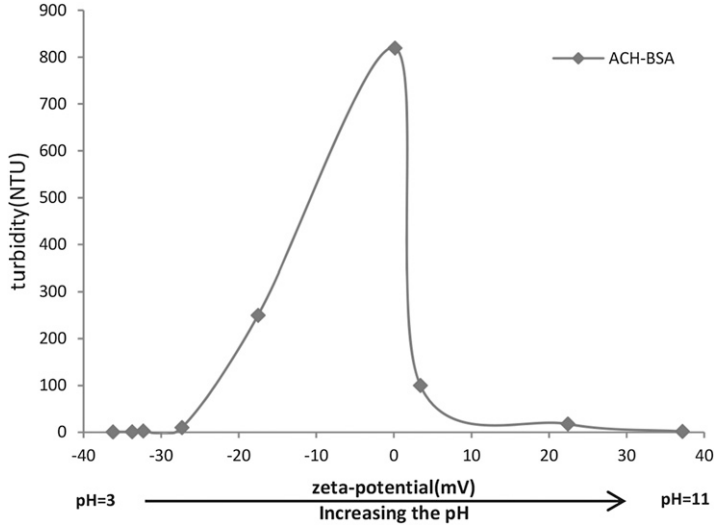

Figure 6. Turbidity of activated ACH-BSA changes as a function of zeta potential with increasing of pH. In all four samples, solutions were transparent at pH = 3, precipitate was observed when pH was raised over 4, at pH between 5 and 6, the largest amount of precipitate was formed, the precipitate dissolved and mixture solution became clear as pH was over 7.

solution as a function of ζ-potential with the increasing of pH. The other three samples had similar behavior in this experiment, and the results are presented in Figure 7. When the pH is less than 4.7, BSA is positively charged. The repulsion between BSA^{+} and Al^{3+} or Zn^{4+} ions leads to transparent solutions. At higher pHs, especially above 5, the solutions were visually cloudy with voluminous precipitate. The largest amount of precipitate was observed at the pH range 5–6. Precipitate started to dissipate when pH was over 8. In ACH–BSA and Al_{13}–BSA solutions, no precipitate was observed when the pH was greater than 9, likely due to the aforementioned formation of $Al(OH)_4^-$. For ZAG and ZG–BSA mixtures, there was a large decreasing in turbidity when the pH was higher than 8. However, these two mixtures still appeared cloudy as expected. Table IV is a summary of the precipitation pH range for AP–BSA samples. The formation of precipitate between BSA and AP salts is found to be a reversible process that is critically dependent on the solution pH. At the pH range of human sweat, around 6, (36) the largest amount of precipitate is expected to form.

COMPARISON AND PREDICTION OF AP EFFICACY BY ZETA POTENTIAL AND TURBIDITY MEASUREMENTS

ASCH, activated ACH, ACH, activated ZAG, ZAG, and three complex molecules, Al_{13}-mer, Al_{30}-mer and ZG were selected to compare the efficacy as AP by using ζ-potential and turbidity measurements of AP–BSA mixtures. Figure 8 shows the ζ-potential change versus the amount of metal salts added. The molar ratio and turbidity at the IEP are two essential parameters to evaluate AP efficacy. Results of this study are shown in Table V.

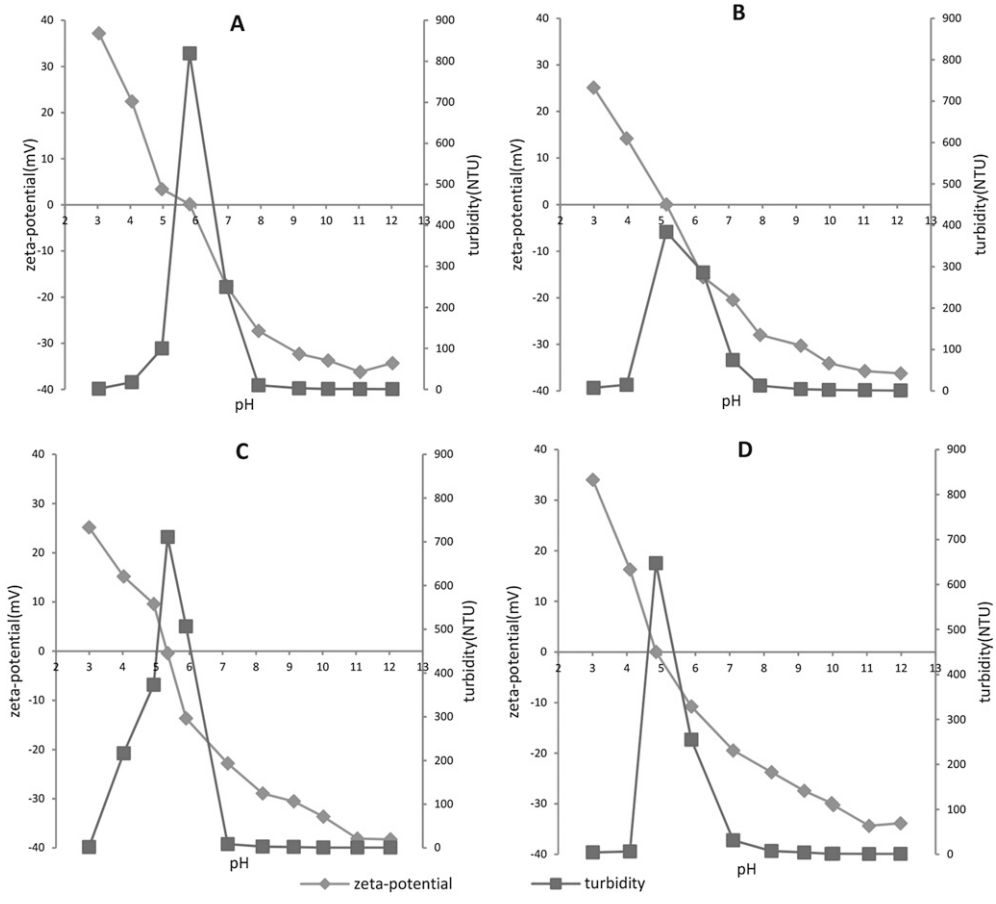

Figure 7. Zeta potential and turbidity trend of AP-BSA mixtures which had largest amount of precipitate with pH change from 3 to 12. (A) Activated ACH-BSA, (B) ZAG-BSA, (C) Al_{13}-BSA, (D) ZG-BSA. In all four samples, solutions were all transparent at pH = 3, precipitate was observed when pH was raised over 4, at pH between 5 and 6, the largest amount of precipitate was formed, the precipitate dissolved and mixture solution became clear as pH was over 7.

It is well known that activated ACH provides much better performance than standard non-activated ACH in sweat inhibition clinical studies. In addition, studies have also shown that ASCH is more efficacious than both activated and regular ACH (35). Comparing the experimental results, ASCH shows the most effective neutralizing capability

Table IV
Precipitation pH Range of AP–BSA Mixture Solutions

Samples	Precipitation pH range
activated ACH	$5 \leq pH \leq 7$
ZAG	$5 \leq pH \leq 7$
Al_{13}	$4 \leq pH \leq 6$
ZG	$5 \leq pH \leq 6$

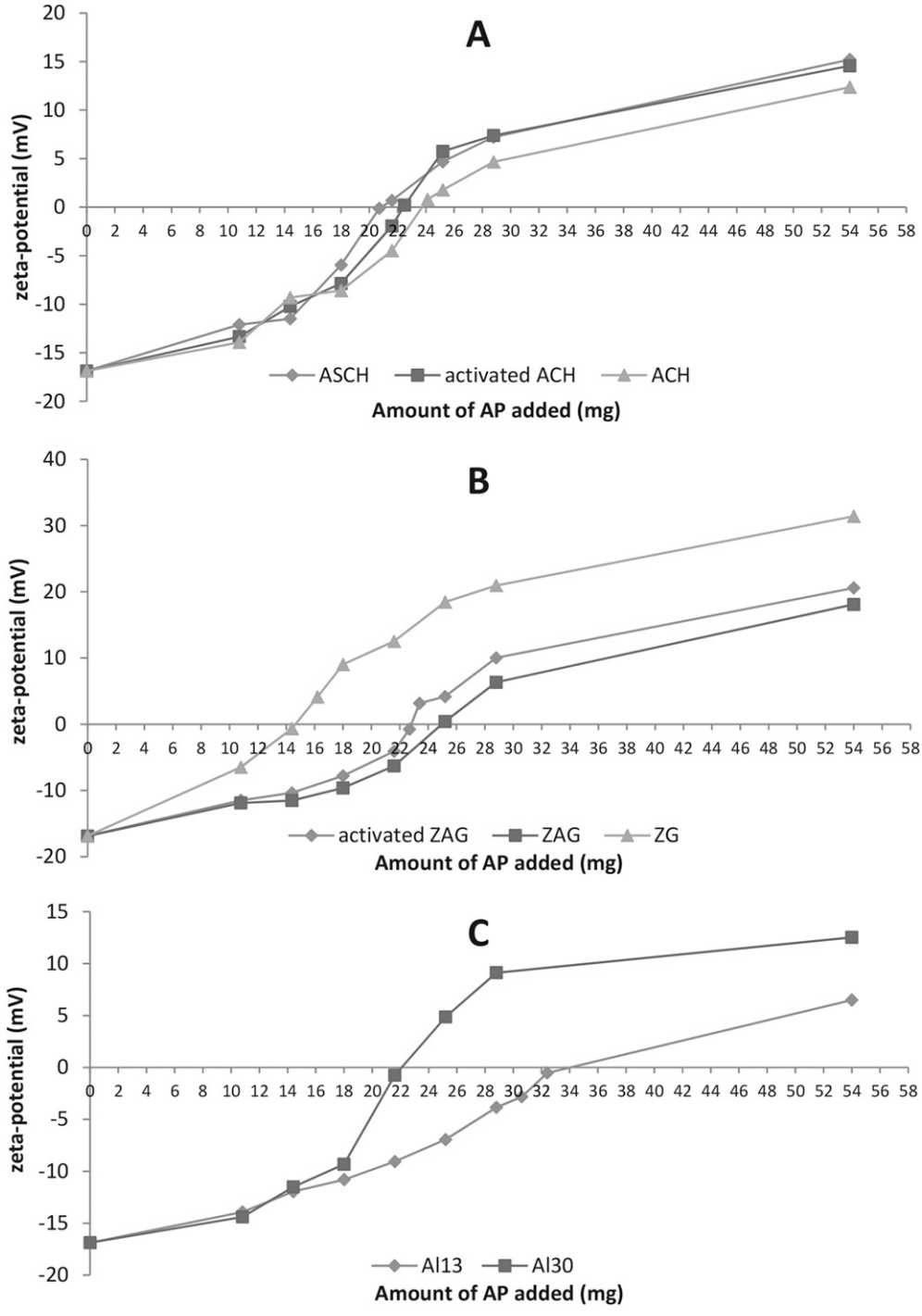

Figure 8. Prediction of AP efficacy by zeta potential measurements. (A) Comparison of Al containing species, (B) comparison of Zr containing species, (C) comparison of Al polyoxocations.

Table V
IEP, Molar Ratio at IEP and Turbidity at IEP of AP–BSA Mixtures

Samples	IEP	Molar ratio at IEP (AP–BSA)	Turbidity at IEP (NTU)
activate ACH	5.61	24:1	549
ACH	5.28	30:1	360
ASCH	5.25	22:1	663
activated ZAG	5.28	7:1	416
inactivated ZAG	5.65	8:1	390
ZG	5.08	3:2	386
Al13-mer-BSA	5.58	4:1	520
Al30-mr-BSA	5.33	3:2	812

and also forms the highest amount of precipitate. Concomitantly, ACH exhibits the lowest performance in terms of both neutralization capability and precipitate formation. In clinical studies, ZAG has been demonstrated to be more efficacious than ACH, activated ACH, and ASCH (36). In comparison to the aluminum-only salts, activated ZAG is expected to work better than standard ZAG. The experimental data corroborates this hypothesis, with activated ZAG achieving higher turbidity at a lower dosing level. Overall, a comparison of commercial AP efficacy by ζ-potential and turbidity measurements provides an order of efficacy as: ACH < activated ACH < ASCH < ZAG < activated ZAG.

ZG (CP-2), a newly developed AP salt reported by our group, performs much better than both activated ZAG and ZAG. The turbidity of ZG–BSA at the IEP falls at the similar level as two other ZAG actives; however, the much lower molar ratio of ZG/BSA at IEP indicates that ZG is the most efficacious salt compared with other commercial actives.

Al_{30}-mer, as an 18+ polycation, would be expected to outperform Al_{13} (7+) in terms of coagulation/flocculation efficacy (40). Chen *et al*. (3,6) has confirmed this expectation. Our experimental data from ζ-potential and turbidity measurements not only supports the better charge neutralization capability of Al_{30} by indicating a low AP/BSA molar ratio, but also confirms the finding from previous studies by showing higher turbidity at the IEP.

Figure 9 is a schematic illustration used to explain the formation of the AP–BSA insoluble adduct at different pH. In zone 1, where the pH is below the IEP of BSA, both AP particles and BSA particles carry positive charges. Therefore, the strong electrostatic

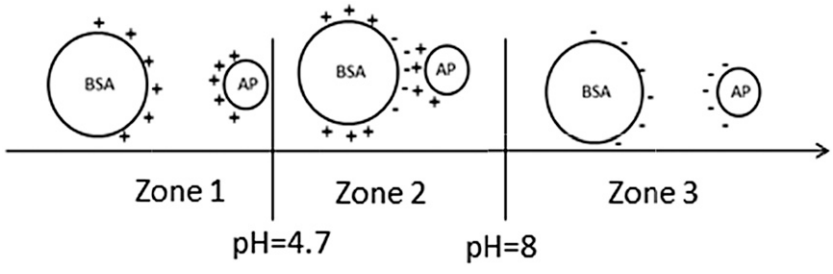

Figure 9. Schematic illustration of the electrostatic interaction between BSA and AP particles in three regions under different pH.

repulsion prevents the adsorption of AP onto BSA. In zone 2, BSA particles are negatively charged while AP particles still carry positive charges; the electrostatic attraction causes adsorption on to the BSA surface. In zone 3, both BSA and AP particles are negatively charged—leading to repulsion between these two particles. The zeta potential measurement technique provides an effective and efficient way to evaluate efficacy of metal salts to use as AP product or coagulants/flocculants in water treatment.

CONCLUSIONS

The possibility of using ζ-potential measurements to demonstrate the optimal interaction between BSA across a wide range of commercial AP actives has been successfully investigated. ζ-potential measurement is not only effective, but can also be used as a simple indicator to evaluate the efficacy of an AP active when it is combined with a solution containing a representative biomolecule (e.g., BSA) at IEP. As a result of minimum repulsion, an insoluble AP–BSA precipitate was formed at the pH where the molar ratio of AP/BSA allows for electrostatic neutrality and the ζ-potential of solution is zero, also known as IEP. The disparity between the turbidity of AP salts alone and turbidity of the AP–BSA combination implicates the importance of biomolecules in the Plug Theory. The electrostatically driven mechanism of plug formation is similar to that which is accepted as the mode of action of primary coagulants in water treatment. The techniques and results described here should allow for more quantitatively analysis of new AP actives, as well as providing insight into the rational design of new active salts.

ACKNOWLEDGMENTS

The authors warmly thank Dr. Andrei Potain from Colgate-Palmolive Co. for helping and providing advice on the operation of Zetasizer.

REFERENCES

(1) J. Duan and J. Gregory, Coagulation by hydrolyzing metal salts, *Adv. Colloid Interface Sci*., **100–102,** 475–502 (2003).
(2) S. D. Faust and O. M. Aly, *Chemistry of Water Treatment*. 2nd Ed. CRC (Press, Boca Raton, 2010), pp. 217–268.
(3) Z. Chen, B. Fan, X. Peng, Z. Zhang, J. Fan, and Z. Luan, Evaluation of Al_{30} polynuclear species in polyaluminum solutions as coagulant for water treatment, *Chemosphere*, **64,** 912–918 (2006).
(4) B. Shi, Q. Wei, D. Wang, Z. Zhu, and H. Tang, Coagulation of humic acid: The performance of preformed and non-preformed Al species, *Colloids Surf*., A, **296,** 141–148 (2007).
(5) C. Staaks, R. Fabris, T. Lowe, C. W. K. Chow, J. A. van Leeuwen, and M. Drikas, Coagulation assessment and optimisation with a photometric dispersion analyser and organic characterisation for natural organic matter removal performance, *Chem. Eng. J*., **168,** 629–634 (2011).
(6) Z. Chen, Z. Luan, Z. Jia, and X. Li, Study on the hydrolysis/precipitation behavior of Keggin Al_{13} and Al_{30} polymers in polyaluminum solutions, *J. Environ. Manage*., **90,** 2831–2840 (2009).
(7) K. Laden, "Antiperspirants and Deodorants: History of Major HBA Market," in *Antiperspirants and Deodorants*. K. Laden. Ed. Cosmetic Science and Technology Series. 2nd Ed. (Marcel Dekker Inc, New York, 1999), pp. 1–14.
(8) C. J. C. Edwards and A. K. Mills, "A Guide to Understand Antiperspirant Formulations," in *Antiperspirants and Deodorants*. K. Laden. Ed. Cosmetic Science and Technology Series. 2nd Ed. (Marcel Dekker Inc, New York, 1999), pp. 233–257.

(9) H. H. Reller, W. I. Luedders, Pharmacologic and toxicology effects of topically applied agents on the eccrine sweat glands, *Mod. Toxicol.,* 4**,** 1–54 (1977).
(10) R. P. Quatrale, A. H. Waldman, J. G. Rogers, and C. B. Felger, The mechanism of antiperspirant action by aluminum salts. I. The effect of cellophane tape stripping on aluminum salt-inhibited eccrine sweat glands, *J. Soc. Cosmet. Chem.*, **32,** 67–73 (1981).
(11) R. P. Quatrale, D. W. Coble, K. L. Stoner, and C. B. Felger, The mechanism of antiperspirant action by aluminum salts. II. Historical observations of human eccrine sweat glands inhibited by aluminum chlorohydrate, *J. Soc. Cosmet. Chem.*, **32,** 107–136 (1981).
(12) R. P. Quatrale, D. W. Coble, K. L. Stoner, and C. B. Felger, The mechanism of antiperspirant action by aluminum salts. III. Historical observations of human eccrine sweat glands inhibited by aluminum zirconium chlorohydrate glycine complex, *J. Soc. Cosmet. Chem.*, **32,** 195–221 (1981).
(13) P. M. Christopher, The action of antiperspirants, *J. Soc. Cosmet. Chem.*, **17,** 789–800 (1966).
(14) R. P. Quatrale, E. L. Thomas, and J. E. Birnbaum, The site of antiperspirant action by aluminum salts in the eccrine sweat glands of the axilla, *J. Soc. Cosmet. Chem.*, **36,** 435–440 (1985).
(15) Z. G. Peng, K. Hidajat, and M. S. Uddin, Adsorption of bovine serum albumin on nanosized magnetic particles, *J. Colloid Interf. Sci.*, **271,** 277–283 (2004).
(16) O. Deschaume, K. L. Shafran, and C. C. Perry, Interactions of bovine serum albumin with aluminum polyoxocations and aluminum hydroxide, *Langmuir*, **22,** 10078–10088 (2006).
(17) O. Deschaume, A. Fournier, K. L. Shafran, and C. C. Perry, Interaction of aluminium hydrolytic species with biomolecules, *New J. Chem.*, **32,** 1346–1353 (2008).
(18) H. B. Yao, Y. X. Yan, H. L. Gao, J. Vaugh, I. Pappas, J. G. Masters, S. Yuan, S. H. Yu, and L. Pan, An investigation of zirconium(IV)–glycine(CP-2) hybrid complex in bovine serum albumin protein matrix under varying conditions, *J. Mater. Chem.*, **21,** 19005–19012 (2011).
(19) D. Yuan, Z. shen, R. Liu, and C. Gao, Study on the interaction of La^{3+} with bovine serum albumin at molecular level, *J. Lumin.*, **131**, 2478–2482 (2011).
(20) F. Wu, L. Zhang, Z. Ji, and X. Wan, Spectroscopic investigation of the interaction between thioureazinc complex and serum albumin, *J. Lumin.*, **130,** 1280–1284 (2010).
(21) P. Rubini, A. Lakatos, D. Champmartin, and T. Kiss, Speciation and structural aspects of interactions of Al(III) with small biomolecules, *Coord. Chem. Rev.*, **228,** 137–152 (2002).
(22) H. H Mosher, Simultaneous study of constituents of urine and perspiration, *J. Biol. Chem.*, **99,** 781–790 (1933).
(23) A. Metes, N. Koprivanac, and A. Glasnovic, Flocculation as a treatment method for printing ink wastewater, *Water Environ. Res.*, **72** (6), 680–688 (2000).
(24) T. Tripathy and B. Ranjan De, Flocculation: A new way to treat the waste water, *J. Phys. Sci.* **10,** 93–127 (2006).
(25) E. L. Sharp, P. Jarvis, S. A. Parsons, and B. Jefferson, Impact of fractional character on the coagulation of NOM, *Environ. Sci. Technol.*, **40,** 3934–3940 (2006).
(26) H. M. Kwaambwa and A. R. Rennie, Interactions of surfactants with a water treatment protein from *Moringa oleifera* seeds in solution studied by zeta-potential and light scattering measurements, *Biopolymers.*, **97**(4), 209–218 (2011).
(27) K. Rezwan, L. P. Meier, M. Rezwan, J. Vörös, M. Textor, and L. J. Gauckler, Bovine serum albumin adsorption onto colloidal Al2O3 particles: A new model based on zeta potential and UV-vis measurement, *Langmuir.*, **20,** 10055–10061 (2004).
(28) P. Wang and A. A. Keller, natural and engineered nano and colloid transport: role of zeta potential in prediction of particle disposition, *Langmuir*, **25** (12), 6856–6862 (2009).
(29) I. Pappas, M. Fitzgerald, X. Huang, J. Li, and L. Pan, Thermally resolved in situ dynamic light scattering studies of zirconium (IV) complex formation, *Cryst. Growth Des*. **9,** 5213–5219 (2009).
(30) B. Shi, G. Li, D. Wang, and H. Tang, Separation of Al_{13} from polyaluminum chloride by sulfate precipitation and nitrate metathesis, *Sep. Purif. Technol.*, **54,** 88–95 (2007).
(31) J. Rowsell and L. F. Nazar, Speciation and thermal transformation in alumina sols: Structures of the polyhydroxyoxoaluminum cluster [Al 30 O 8 (OH) 56 (H 2 O) 26] 18+ and Its δ-Keggin Moieté, *J. Am. Chem. Soc.*, **122,** 3777–3778 (2000).
(32) L. Allouche, C. Gérardin, T. Loiseau, and G. Férey, F. Taulelle, Al(30): A giant aluminum polycation, *Angew. Chem. Int. Ed.*, **39**(3), 511–514 (2000).
(33) Malvern Instruments Ltd, "Zeta Potential theory," in *Zetasizer nano series User Manual*, England, pp. 16-1-16-12.
(34) T. Peters, *All About Albumin: Biochemistry, Genetics, and Medical Applications*, (Academic Press: San Diego, 1996).

(35) J. J. Fitzgerald and A. H. Rosenberg, "Chemistry of Aluminum Chlorohydrate and Activated Aluminum Chlorohydrates," in *Antiperspirants and Deodorants*, K. Laden. Ed. Cosmetic Science and Technology Series. 2nd Ed. (Marcel Dekker Inc, New York, 1999), pp. 83–136.
(36) A. H. Rosenberg and J. J. Fitzgerald, "Chemistry of Aluminum-Zirconium-Glycine (AZG) Complexes," in, *Antiperspirants and Deodorants*, K. Laden. Ed. Cosmetic Science and Technology Series. 2nd Ed. (Marcel Dekker Inc, New York, 1999), pp. 137–168.
(37) P. Benezeth, D. A. Palmer, and D. J. Wesolowski, The aqueous chemistry of aluminum. A new approach to high-temperature solubility measurements, *Geothermics*, **26,** 465–481 (1997).
(38) V. Pophristic, M. L. Klein and M. N. Holerca, Modeling of small aluminum chlorohydrate polymers, *J. Phys. Chem. A.*, **108,** 113–120 (2004).
(39) D. L. Teagarden and S. L. Hem, Conversion of aluminum chlorohydrate to aluminum hydroxide, *J. Soc. Cosmet. Chem.*, **33,** 281–295 (1982).
(40) I. M. Metcalfe and T. W. Healy, Charge-regulation modelling of the Schulze–Hardy rule and related coagulation effects, *Faraday Discuss. Chem. Soc.*, **90,** 335–344 (1990).